J Mol Model (2007) 13:559–572
DOI 10.1007/s00894-007-0178-7

ORIGINAL PAPER

Long-time molecular dynamics simulations of botulinum biotoxin type-A at different pH values and temperatures

Xin Chen · Yuefan Deng

Received: 3 November 2006 / Accepted: 26 January 2007 / Published online: 27 February 2007

Abstract Botulinum neurotoxins type A (BoNT/A) are highly potent toxins, but are also useful in the treatment of illnesses. We studied the properties of BoNT/A at various temperatures and pH values in order to understand its toxicity and structure variations. The pH values of the environment of BoNT/A are obtained by changing the protonation states of certain titratable residue groups. Our results show that certain parts of the protein are active at acidic pH environments or at high temperatures. The protein is more stable in neutral environments at normal human body temperature, whereas, at high temperature, the protein is more stable in acidic environments. Also, the three domains of the protein tend to have relative motion rather than within individual domains.

Keywords Botulinum toxin · Constant pH molecular dynamics · Protein folding

Introduction to Botulinum

Botulinum neurotoxins (BoNT) are among the most toxic proteins to humans. They are about 100 billion times [1] more toxic than cyanide. They have seven different serotypes (BoNT/A–BoNT/G), each produced by different strains of Clostridium botulinum.

The BoNT we study in this paper is of type A (BoNT/A). We studied the properties, and the mechanism of the toxicity, of BoNT/A in a low pH environment. Such properties and mechanism, elusive at the present time, are important to understand because a low pH environment plays a very important role in the process of the reaction of BoNT/A with cells.

Like most known poisonous substance, Botulinum toxin can be used as a biological weapon [2, 3]. Only about 10^{-7} g BoNT/A can kill a person, which means that a single gram of crystalline toxin, evenly dispersed and inhaled, can kill more than one million people. Although BoNT/A is among the most toxic proteins to humans, purified botulism toxin is the first bacterial toxin to be used as medicine. The FDA licensed botulinum toxin as "Oculinum" in December 1989 for treating two eye conditions—blepharospasm [4] and strabismus [5]—characterized by excessive muscle contractions. It is now marketed under the trade name Botox and is widely used for cosmetic purposes to remove wrinkles [6]. It is also used to treat blepharospasm, strabismus, and cervical dystonia [7]. Other applications for Botox are currently under investigation. It has been reported that spasmodic dysphonia, a neurological disorder that affects the muscles of the larynx, responds well to Botox treatment [8]. It has also been used to treat other dystonias, such as writer's cramp, as well as facial spasms, head and neck tremors and hyperhidrosis. A recent study [9] has even been conducted to observe its use in treating chronic neck and back pain.

The toxicity of BoNT/A is proposed as a result of a four-step mechanism: [1] extracellular binding, internalization, membrane translocation, and intracellular blockage of

X. Chen
Department of Physics, Stony Brook University,
Stony Brook, NY 11794, USA
e-mail: xinchen@ic.sunysb.edu

Y. Deng
Department of Applied Mathematics,
Stony Brook University,
Stony Brook, NY 11794, USA

Y. Deng (✉)
Institute of Scientific Computing, Nankai University,
300071 Tianjin, People's Republic of China
e-mail: Yuefan.Deng@StonyBrook.edu

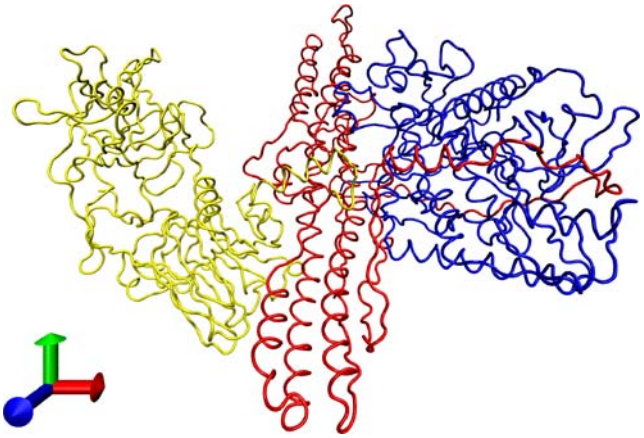

Fig. 1 Domain structures of BoNT/A. *Yellow* binding domain; *red* translocation domain; *blue* catalytic domain

Table 1 Summary of parameters for all numerical experiments

Temperature	pH values	
	pH 4.7	pH 7.0
37 °C	Whole protein (~64 ns)	Whole protein (~63 ns)
	LC only (200 ns)	LC only (200 ns)
55 °C	Whole protein (~57 ns)	Whole protein (~67 ns)
	LC only (200 ns)	LC only (200 ns)

acetylcholine release. In the first step, the BoNT/A binds to the pre-synaptic nerve endings of cholinergic neurons through protein receptors on unmyelinated presynapitc membrane. This process is mediated by the binding domain of BoNT/A. In the second step, the BoNT/A is internalized by receptor-mediated endocytosis. After that, the low pH inside the endosome is believed to trigger a membrane pore formation by the heavy chain (HC), by inducting exposure of the hydrophobic polypeptide segment in the translocation domain. In this process, HC forms a channel, which allows translocation of at least the light chain (LC) across the endosomal membrane into the cytosol. Low pH in endosomes is very important in this process; it is believed to cause conformation changes in the translocation domain to form the channel. The third step is the translocation of LC across the endosome membrane from lumen of endosome to cytosol. In this process, the HC and LC become separated after reduction of the disulfide bond. However, the size of the pore formed by HC has been estimated to be about 8 Å, which is too small to accommodate the 50 kDa LC. It has been speculated that the low pH could cause conformational change of the LC so that it can be accommodated in the HC pore. When it reaches cytosol, a more neutral pH will restore LC structure. In the final step, the LC specifically cleaves the synaptosomal protein of 25 kDa, SANP-25, through its Zn^{2+}.

As with the most toxic proteins, it is difficult and dangerous to handle BoNT/A for conducting traditional laboratory experiments, making computational simulation a necessity. However, simulating large proteins like BoNT/A is extremely challenging even for very large supercomputers, due to the need to simulate for long time scales. Until now, there is no known report for modeling BoNT/A to long time scales. Our simulation was done on the Beowulf cluster NankaiStars [10] at Nankai University in China with 800 Intel Xeon processors running at 3.06 GHz. A typical run of our protein with a typical configuration

Fig. 2 Titration curve

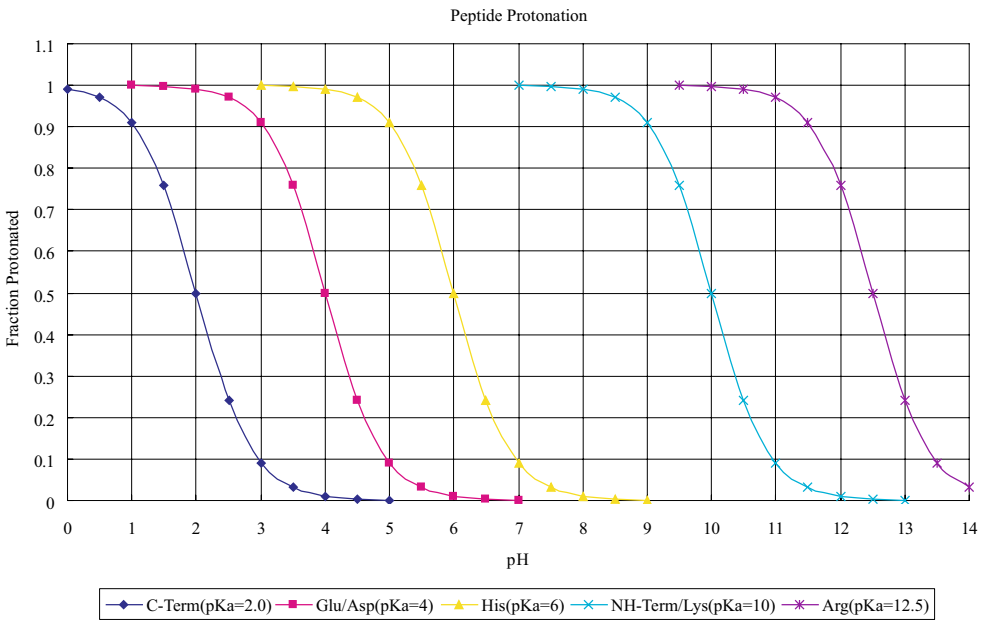

Table 2 Running speed on the Nankai Stars Beowulf computer

Number of CPUs	Running speed (ns/day)	Speed-up
32	0.27	32
64	0.63	74
128	1.16	137
256	2.01	238
512	2.95	350

The seemingly super speedup for the cases of 64 and 128 CPUs may result from heavy virtual memory accesses for 32-CPU case. For our protein, it fits well on 64 CPUs. Of course, for systems with more CPUs (256 and 512), communicate slows systems down

takes 3 months to achieve 100 ns physical time at a rate of about 1 ns/day on a 128-nodes portion of the machine.

Protonation states of titratable residue were changed to simulate an acidic pH environment for BoNT/A in this paper. This method was used to verify another method proposed by Mongan et al. [11] to simulate the constant pH value as in AMBER [12] version 8. BoNT/A was simulated at two different temperatures: the normal human body temperature of 37 °C and a higher temperature of 55 °C at which temperature spectacular structure changes were observed by a researcher [13]. And it was also simulated at two different pH values, the neutral one of pH 7.0 and an acidic one of pH 4.7, to study the influence of acidic environment on BoNT/A at the two temperatures. We also simulated the LC of BoNT/A at 37 °C at a pH of 4.7 to study its conformational change at this environment after being cleaved from the HC.

BoNT/A is synthesized in Clostridium botulinum as a ~150 kDa single chain protein with 1,295 amino acids, which are cleaved endogenously or exogenously resulting in a 100 kDa HC and a 50 kDa LC linked through a disulfide bond. It is composed of three ~50 kDa functional domains: [13, 14] the catalytic domain which is confined to the ~50 kDa LC, the translocation domain which is confined to the N-terminal half of the ~100 kDa HC, and the receptor binding domain which is confined to the C-terminal half of HC. They are indicated in different colors in Fig. 1. The dimensions of BoNT/A molecules [15] are approximately $45\times105\times130$ Å^3, the overall dimensions for binding domain are $32\times37\times76$ Å^3. For the translocation domain are $28\times32\times105$ Å^3, while for the catalytic domain are $55\times55\times62$ Å^3.

In our experiments, the structure variations of each domain were studied at different pH values and temperatures. The rest of the paper is organized as follows: modeling methods; simulation results and analysis; further discussions and conclusions.

Table 3 The difference between the systems used for the simulations of BoNT/A at high and low pH values

	Neutral pH (pH 7)	Acid pH (pH 4.7)
Histidine side chains	Not protonated	Protonated
Overall protein charge	−9	+3
Zinc ion	Present	Present
Bounding box	106×120×158	106×120×158
Volume (Å$^{3)}$	2,023,840	2,023,840
Total number of atoms	173,549	173,561
Protein atoms	20,698+Zn^{2+}	20,710+Zn^{2+}
Water molecules	50,950	50,950
Total mass	1,065,388 Da	1,065,400 Da
Total density	0.874 g/cc	0.874 g/cc

Table 4 Simulation time needed

Name	No. of residues	Simulation time
Villin headpiece (alpha helical protein)	36	~10 ms 35/100 has conformational change in 1 ms simulation
Trp-cage	20	~100 ns at 315 K
Beta hairpin	54	38 ms at 300 K
BoNT/A	1,277	Unknown
BoNT/A LC only	431	Unknown

Methods

The structure data file of BoNT/A was obtained from Protein Data Bank (PDB) [16]. The parameter files, the coordinate file (crd file) and the topology file (top file) needed by NAMD [17] were generated in AMBER version 7. The force field used was AMBER force field ff99 [18]. The NAMD performs the molecular dynamics simulations, generating the results in dcd files, with which the Root Mean Square Deviation, or RMSD, values for BoNT/A were calculated using VMD [19]. All simulations were performed in the presence of explicit solvent, TIP3PBOX water model, at different temperatures. Since Zn^{2+} plays an important role for its toxicity, it was included in all simulations.

Table 5 Differences between the systems used for the simulations of LC for pH 4.7 at 37 °C

	Cut-off run	Whole protein run
Total atoms	59,672	173,561
Protein atoms	6,958+Zn^{2+}	20,710+Zn^{2+}
Water molecules	17,571	50,950

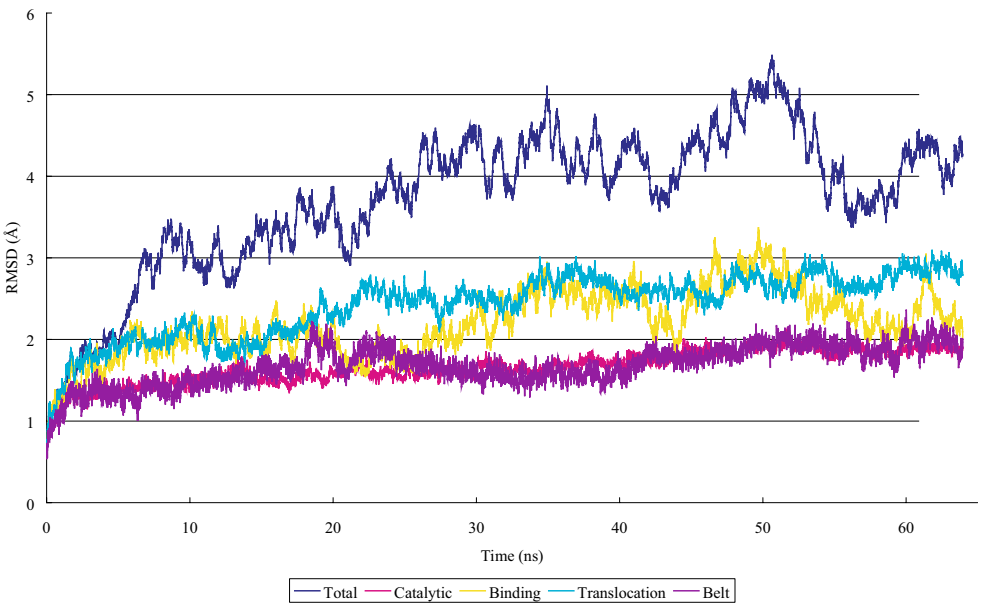

Fig. 3 RMSD of BoNT/A for pH 4.7 at 37 °C

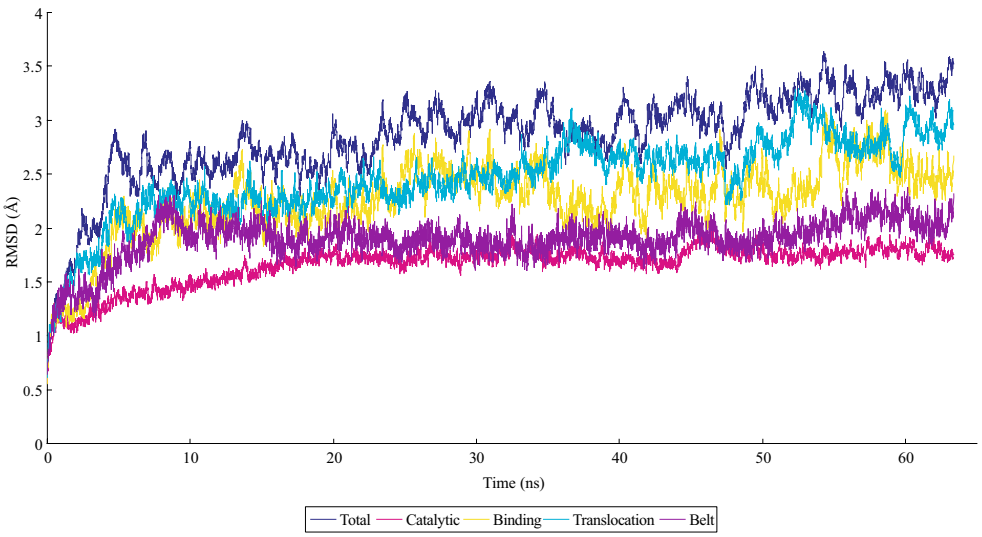

Fig. 4 RMSD of BoNT/A for pH 7.0 at 37 °C

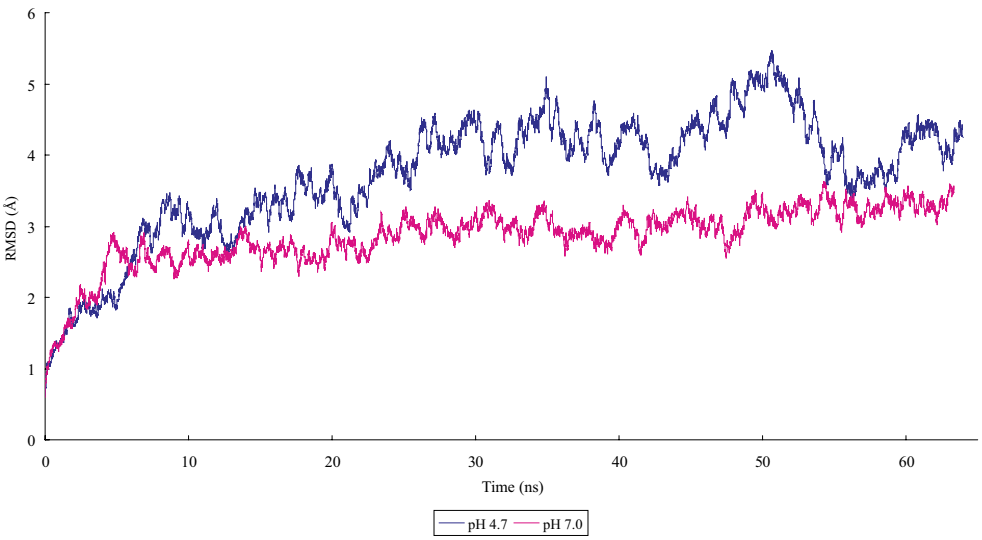

Fig. 5 Comparison of the RMSD for the whole protein at 37 °C

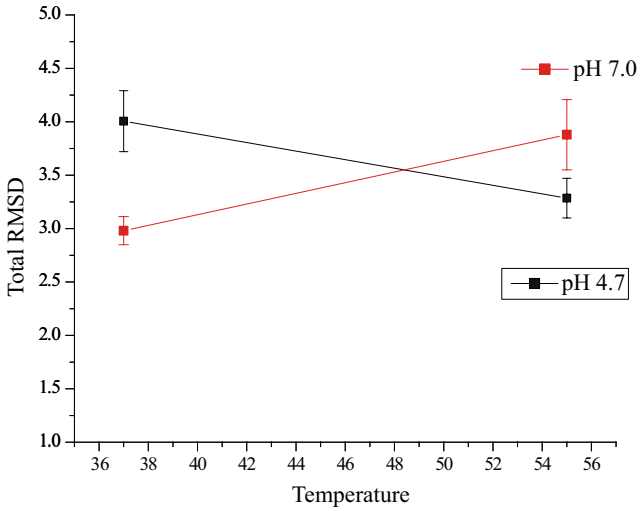

Fig. 6 Comparison of the RMSD for the whole protein

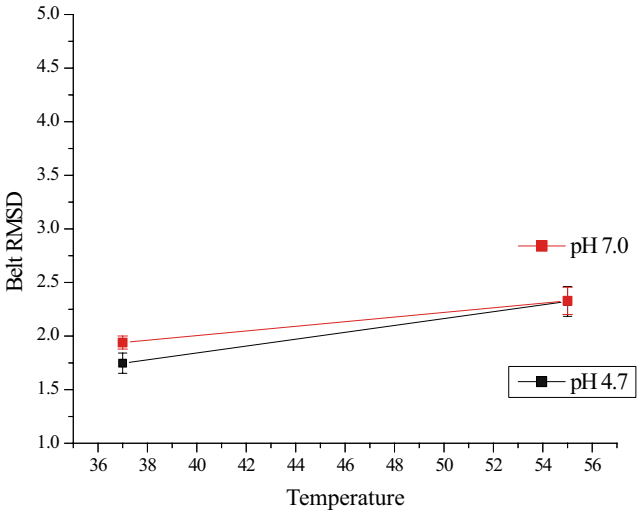

Fig. 8 Comparison of Belt RMSD

The AMBER force field we adopt is

$$V = \frac{1}{2}\sum_{bonds}\left(K_b(b-b_0)^2\right) + \frac{1}{2}\sum_{angles}\left(K_\theta(\theta-\theta_0)^2\right) + \frac{1}{2}\sum_{dihedrals}\left(K_\phi(1+\cos[n\varphi-\gamma])\right) + \sum_{nonbonded}\left[\frac{A}{r^{12}}-\frac{B}{r^6}\right] + \sum_{nonbonded}\frac{q_1q_2}{\varepsilon\, r}$$

Two classes of simulations were run, modeling conditions of high (pH 7.0) and low pH (pH 4.7), respectively. The method used to model the pH values was to change the protonation states of the residues. According to the pKa values of all the titratable residues (Fig. 2), varying the pH values from pH 7.0 to pH 4.7 requires protonation states of Histidin (HIS) residues to change. While the protonation states of other residues mostly remains unaffected. The BoNT/A contains 12 HIS residues; we changed protonation states of them in low pH simulations.

Results and analysis

We used RMSD to analyze the extent to which the system has moved from equilibrium. It characterizes the amount by which a given selection of the molecule deviates from a defined position.

For the analysis of BoNT/A structure at various pH values, we obtained the RMSD by calculating the deviation of the molecule structure at a certain time compared to the initial structure. RMSD values were calculated for all atoms of the protein backbone (without hydrogen) for the entire

Fig. 7 Comparison of RMSD for the belt part

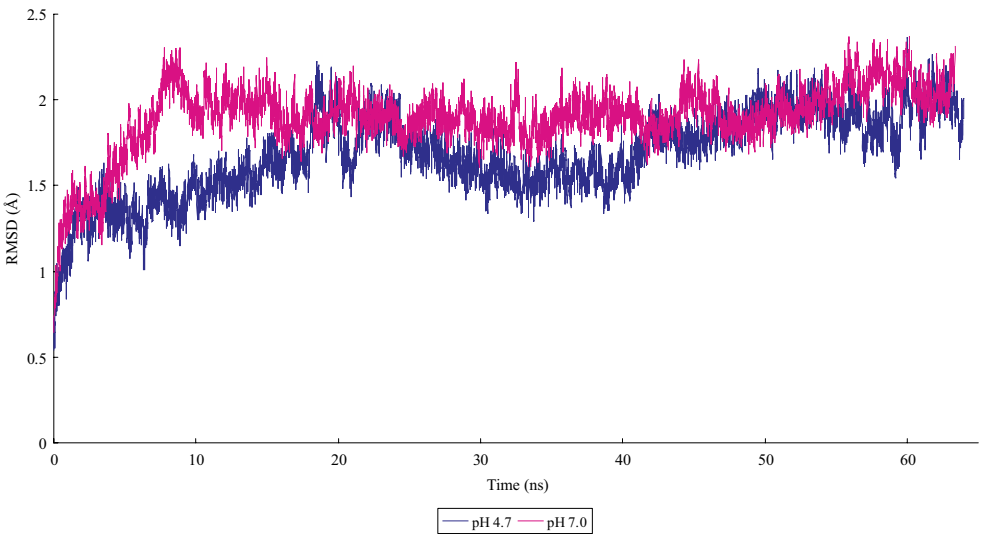

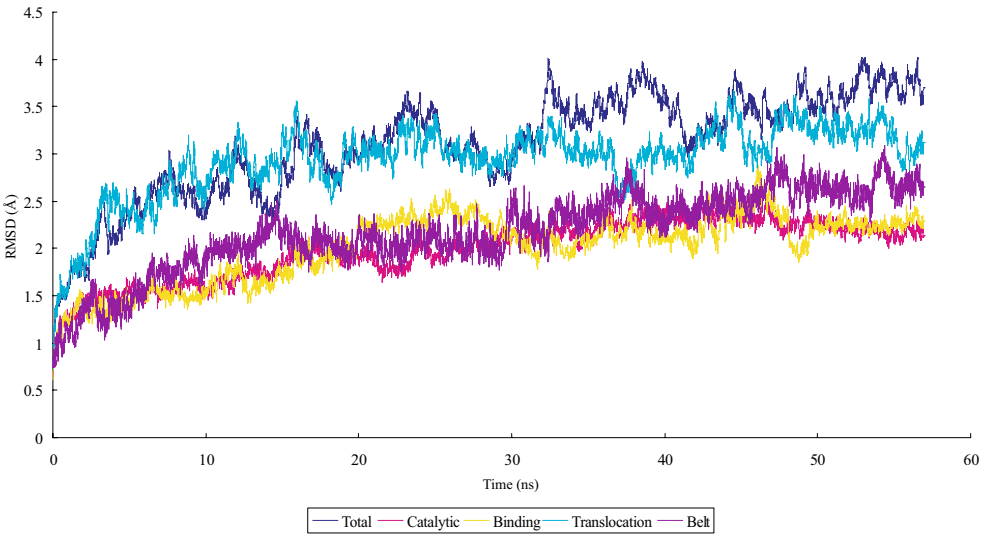

Fig. 9 RMSD of BoNT/A for pH 4.7 at 55 °C

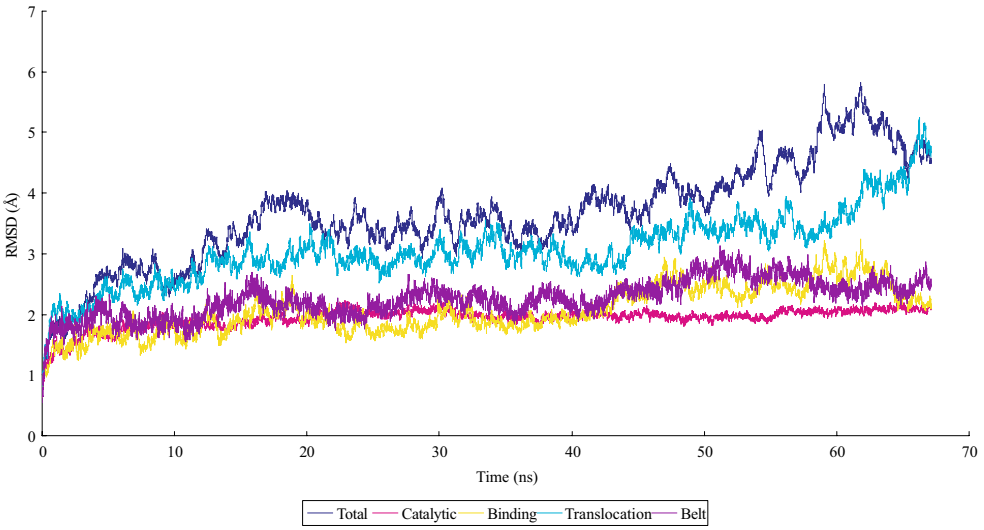

Fig. 10 RMSD of BoNT/A for pH 7.0 at 55 °C

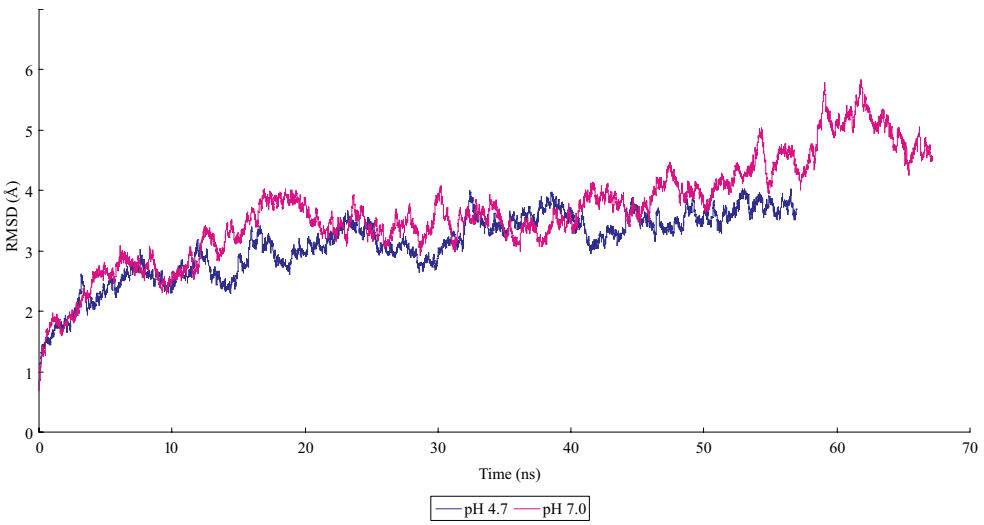

Fig. 11 Comparing of RMSD for the whole protein at 55 °C

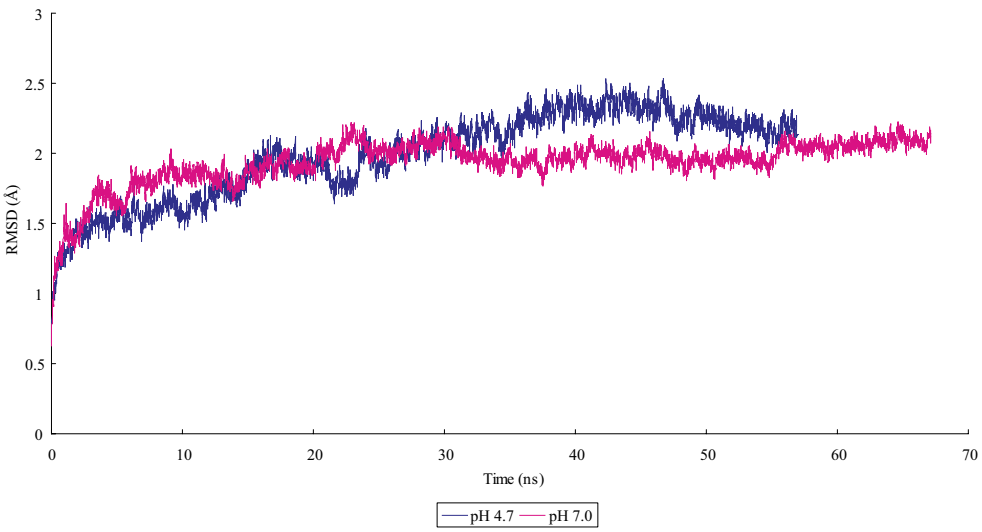

Fig. 12 Comparing of RMSD for the LC at 55 °C

protein. In the analysis, RMSD for the belt part was also included with the RMSD for the whole protein and its three domains. The belt part belongs to the translocation domain and is a long loop that wraps around the catalytic domain, as though to keep the catalytic domain in position. It plays an important role in shielding the active site [14].

The summary of all experiments we conducted is recorded in Table 1; simulations were performed at two temperatures: 37 °C and 55 °C. Two pH values were chosen for our simulations, a neutral one of pH 7.0, and an acidic one of pH 4.7, which is the pH value at which many biological experiments were conducted with speculation that interesting phenomena may occur. For the pH 4.7 at 37 °C experiments, we also had a special simulation by cutting off the LC of BoNT/A and simulating it separately to help understand its mechanism of toxicity. The running speed for the simulation at NankaiStars is in Table 2. The Table 3 shows the details of and the difference between the systems used for the simulations of BoNT/A at high and low pH values.

Table 4 shows various other simulations of proteins before our simulation [20–22] to understand the time scales needed to simulate a protein based on its molecular weight. For small proteins with ~100 residues, a simulation time of about ~10 ms is needed. For large proteins like BoNT/A, no similar simulations were done. However, it can be logically inferred that a simulation timescale in the order of microseconds is needed.

Constant pH simulation at human body temperature, 37 °C

Figures 3 and 4 show the RMSD of BoNT/A and its three domains as a function of time at pH 4.7 and pH 7.0 at a temperature of 37 °C. The RMSD of the belt part is also shown. From these two figures, we find that the RMSD of the belt part oscillates the most, which suggests that it is the most flexible part of the translocation domain. Figure 5 compares the RMSD of the whole protein at two pH values. From this, we can see that the BoNT/A have larger RMSD at the low pH environment, which indicates that the BoNT/A may have some conformation changes at pH 4.7.

To see it more clearly, Fig. 6 was made as follows; the point indicated the average RMSD and the deviation of it for the protein at pH 4.7 and pH 7.0 at 37 °C and 55 °C.

Table 6 System energies at different simulation runs

Energy type	Whole protein runs				LC-only runs			
	pH=4.7		pH=7.0		pH=4.7		pH=7.0	
	37 °C	55 °C	37 °C	55 °C	37 °C	55 °C	37 °C	55 °C
Electrostatic	−764,697	−742,867	−763,152	−743,267	−260,790	−253,214	−289,085	−281,354
Van der Waals	103,152.6	98,585.82	103,218.3	98,659.32	35,578.51	33,868.65	39,918.68	38,116.36
Kinetic	160,470.3	169,786.6	160,468.4	169,769.8	55,178.69	58,372.74	60,769.59	64,296.34
Total	−366,799	−337,423	−365,025	−337,851	−124,229	−114,320	−138,575	−128,117

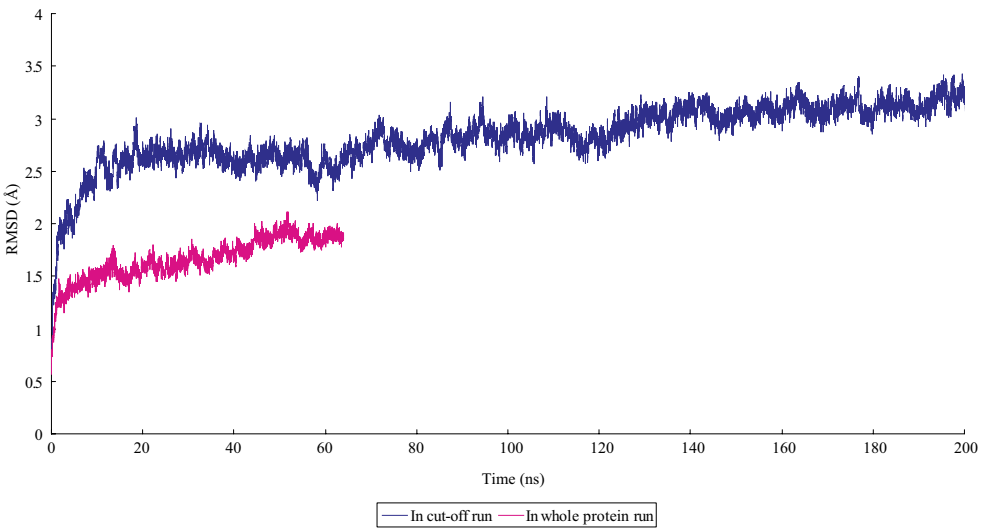

Fig. 13 Cut-off simulation for LC for pH 4.7 at 37 °C

From it, we can see that BoNT/A has different behaviors at different pH values. In an acidic environment, the RMSD of the total protein tends to decrease as temperature increases, while in the neutral environment, the RMSD of the total protein increases with increasing temperature. This may imply that BoNT/A is more stable and temperature resistant at an acidic environment. Figure 7 shows the comparison of the RMSD for the belt part. We can see that the RMSD is higher at pH 7.0 than at pH 4.7.

Using the same method as we did for Fig. 6, we have Fig. 8. It may imply that the conformation of belt part changes more with increasing temperature in low pH environment. Also, the RMSD of the belt part have different values at 37 °C since their error bars do not cross, which implies that, at this temperature, different pH values have a great effect on the structure of the belt part.

Constant pH simulation at higher temperature, 55 °C

Li et al. [13] found that, at a temperature of about 55 °C, the LC denatures at pH 7.0 while remaining stable at low pH 4.7. Their results of temperature-dependent unfolding of LC at pH 7.0 and pH 4.7 as monitored by the near-UV circular dichroism band at 280 nm is shown in Fig. 5 of their paper. Simulations of BoNT/A at 55 °C were conducted to examine these properties at this temperature. The RMSD results are shown in Figs. 9 and 10. From Fig. 11, comparing RMSD for the whole protein at 55 °C, we find

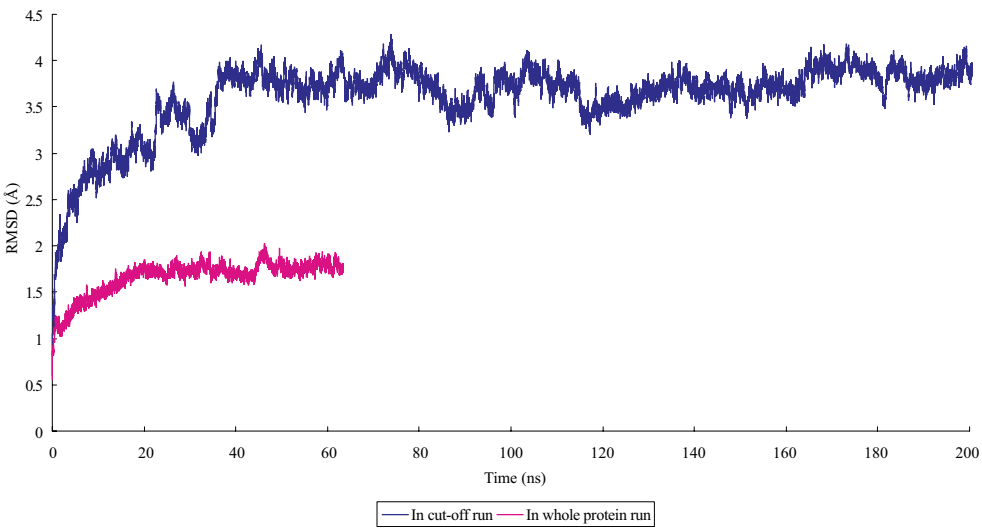

Fig. 14 Cut-off simulation for LC for pH 7.0 at 37 °C

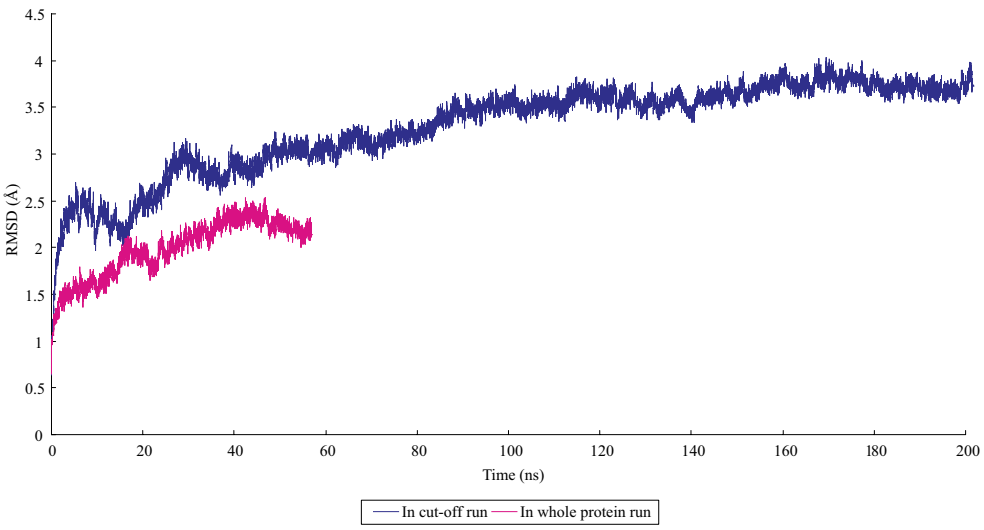

Fig. 15 Cut-off simulation for LC for pH 4.7 at 55 °C

that the RMSD at pH 4.7 is lower than at pH 7.0, which support the idea that the whole protein is more stable in an acidic environment than in a neutral environment. Figure 12 shows the comparing of RMSD for the LC at 55 °C. From it, we can see that, although RMSD for the LC at pH 4.7 is lower than that at pH 7.0 before 15 ns, they cross after that time. We expect that longer simulations would verify the claims by Li et al. [13] of LC at 55 °C.

Cut-off simulation of LC at human body temperature, 37 °C

It is believed that the LC is only active after reduction of the disulfide bonds [1]. The LC of BoNT/A neurotoxin will undergo autocatalytic fragmentation that is accelerated by the presence of the metal cofactor, zinc [23]. It is possible that the low pH triggers a conformational change that forms the LC transporter channel, which must fit within the membrane bilayer (~30 Å). The whole process is still redundant not clear. Some suggest that the translocation of the BoNT/A LC may occur through a mechanism other than the membrane channel formed by the BoNT/A HC. In a "cleft model", the interaction of the BoNT/A LC directly with lipid bilayer has been proposed [24]. To understand this process, we simulated the LC after it had been cut off from other part of the protein with a Zn ion.

The LC contains six HIS residues which changed the protonation states during the pH change. The net charge of the LC is −1 not including the Zn^{2+} at pH 7.0 (Histidin not protonated), and 5 not including the Zn^{2+} at pH 4.7 (Histidin protonated). Table 5 shows the differences

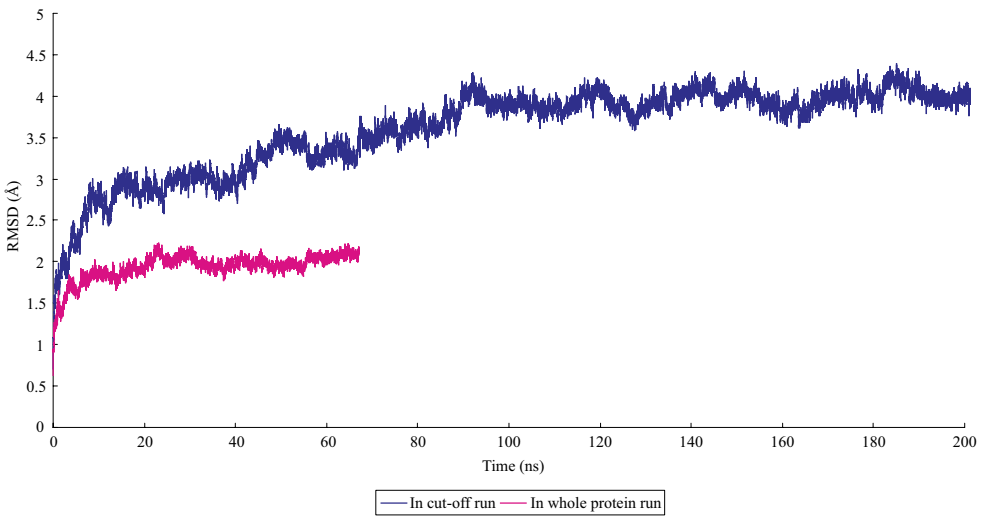

Fig. 16 Cut-off simulation for LC for pH 7.0 at 55 °C

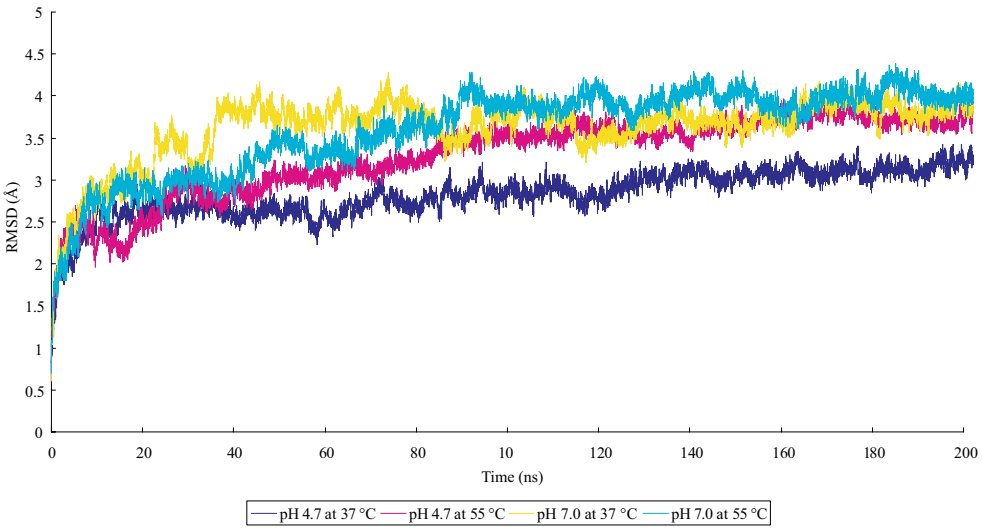

Fig. 17 Cut-off simulation for LC at different pH and temperatures

between the systems used for the simulations of LC for pH 4.7 at 37°C. For LC-only runs, the number of atoms is about 1/3 of the whole protein run, which greatly increased the simulation speed. With 64 processors at NankaiStars, we can get about 1.2 ns physical time per day, compared to 0.5 ns per day for the whole protein run. This is very important for us, since the possible conformational change occurs over a long time scale.

The result for 4.7 at 37 °C is shown in Fig. 13. From it, we can see that the RMSD of cut-off LC is significantly higher than the normal run. This is very important since, for the mechanism for BoNT/A's toxicity, the LC is released from the HC belt after disulfide reduction, thereby making the active site accessible to the substrate. Our results imply that the LC will have a conformational change after being released, which supports the experimental expectation.

We also have results for LC only for pH 7.0 at 37 °C in Fig. 14. We can see that the RMSD of the LC is significantly higher after being cut off. This also makes it clear that the LC's activity depends on it being cu -off from the other part of the protein.

Cut-off simulation for LC at higher temperature, 55 °C

Figures 15 and 16 show the LC-only results compared with the normal runs at a higher temperature, 55 °C. In Fig. 17, we compared the RMSD for LC after being cut off at different pH and temperatures. From this graph, we can see

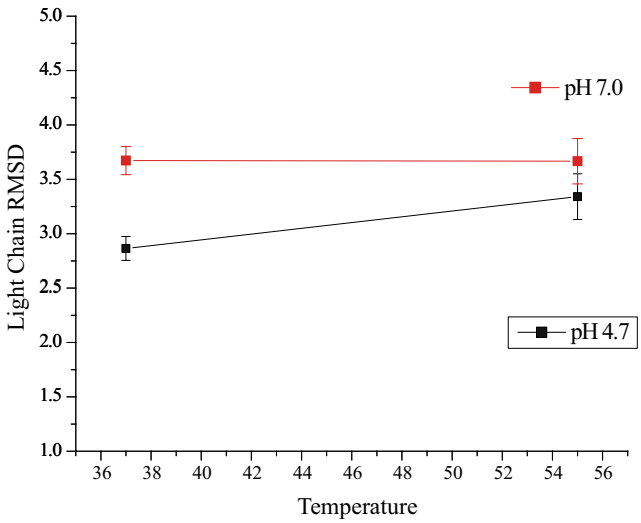

Fig. 18 Comparison of RMSD of LC-only runs

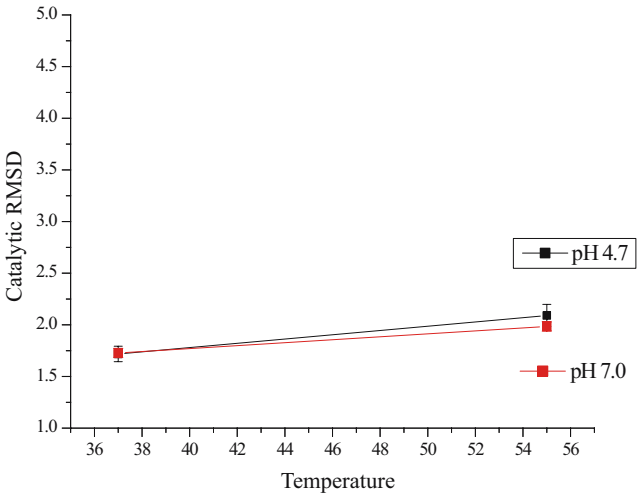

Fig. 19 Comparison of RMSD of catalytic domain in whole protein runs

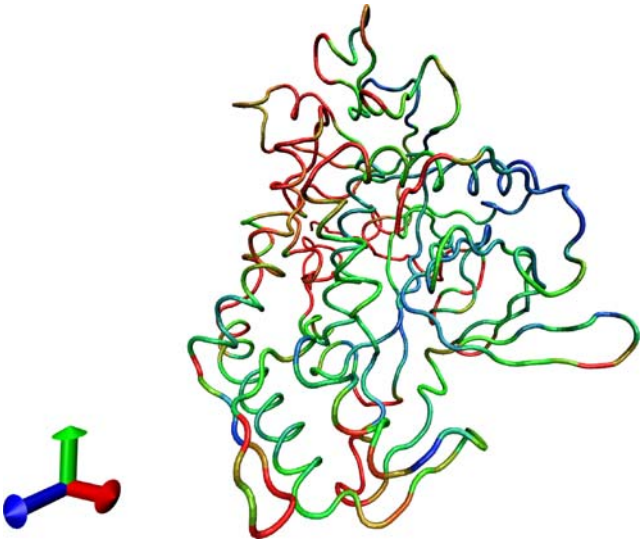

Fig. 20 Comparing of LC-only run and whole protein run

that, at 55 °C, the pH 4.7 run (the red one) has a lower RMSD than the pH 7.0 run (the light blue one), which is what we expected: [13] the acidic environment makes the protein more stable at high temperature. While at 37 °C, the pH 4.7 run (the blue one) also has a much lower RMSD than the pH 7.0 run (the yellow one). It may indicate that, at these two temperatures, the LCs are more stable at an acidic environment than at a neutral environment.

With the same method used in drawing Fig. 6, we obtained Fig. 18 for RMSD of LC-only runs and Fig. 19 for RMSD of catalytic domain in whole protein runs. From these two figures, we can see significant differences. Generally, they have larger RMSD values when running alone than running as part of the protein. Also, as temperature increases, they become more stable, while in the whole protein run, the situation is contrary and their RMSDs became larger with increasing temperatures. There must be some conformational change for the LC after it has been cut off and run separately.

To find the difference, we compared the configuration for two structures in the LC-only run and whole protein run at the same time. Figure 20 shows the deviation of these two structures. The red part means the largest conformational change. From the graph, we can see that the edge part of the LC has a higher deviation. It can be inferred from the graph that after the LC is cut off from the protein, its conformational change starts from its edge part and, as time goes on, it eventually causes the denaturation of the whole LC.

Low frequency phenomena

Oscillations of binding and catalytic domain during the simulation were observed in our simulations, especially in the Y and Z directions. Figure 21 shows the distances between center of mass of each domain to that of the whole protein. This also confirms the conservation of momentum. In addition, this explains why there are some peaks on the RMSD of total protein, while the RMSD of the three domains are stable, like the peak at 59.05 ns in Fig. 10.

Energy analysis

Figure 22 shows a typical relationship between time and the system energy, from which we can see that the system energies are quite stable after a few thousand time steps. So the average energies were calculated and used to determine the properties of the whole system. The electrostatic energy,

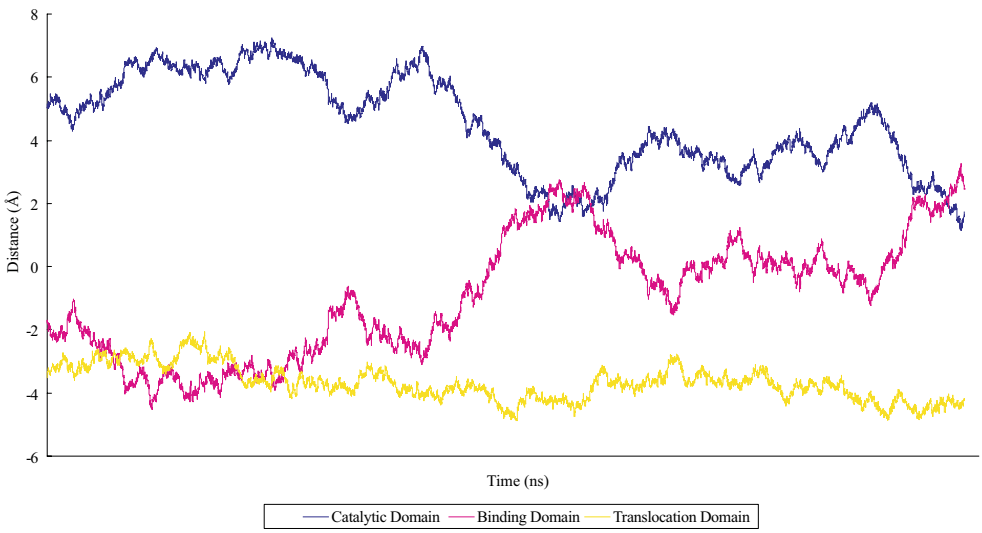

Fig. 21 Low frequency oscillation in Z direction for pH 7.0 at 55 °C

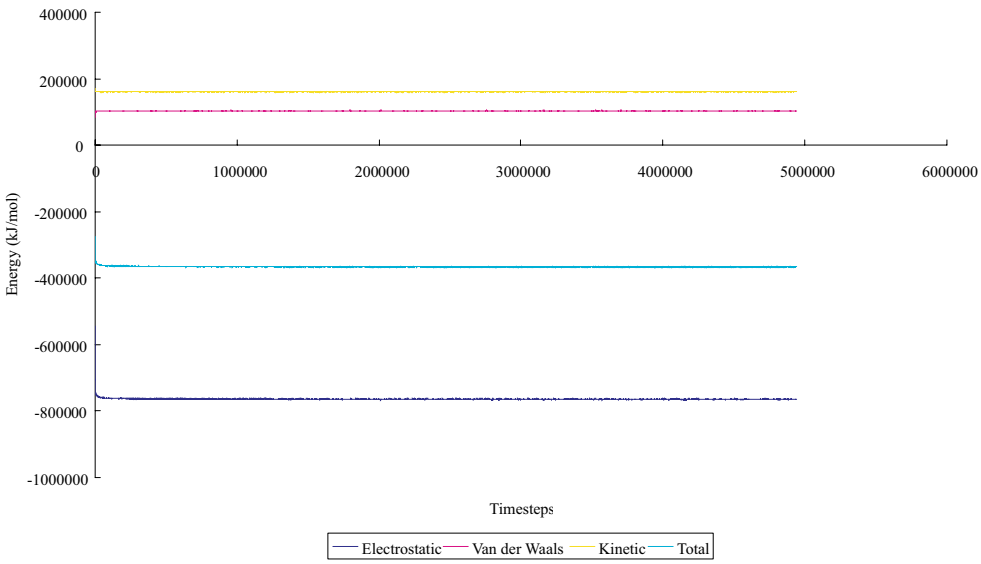

Fig. 22 System energy versus time

van der Waals energy, kinetic energy and the total energy were calculated. All energies are given in kJ mol^{-1} and are listed in Table 6.

We can see that, for the whole protein run, changing the pH does not affect the electrostatic energy at 37 °C and 55 °C. One possible reason is that for the whole protein run, despite the difference of total charges of the protein molecule (−9 at pH 7.0 and +3 at pH 4.7), the whole electrostatic energy is not affected because the titrated HIS residues does not act with others. For the LC-only runs, the situations are different. The changing pH has the same effect of the electrostatic energy despite the temperature. It confirms our expectation that the LC starts conformational change after it has been cut off from the HC. Also, the low pH has a larger electrostatic energy because the system has six more charges at low pH.

For the van der Waals energy at different pH and temperatures, we can see that the situation is very similar: for whole protein runs, changing the pH does not affect the energy at 37 °C and at 55 °C. For LC-only runs, changing pH has the same effect on the energy despite the temperature. In the kinetic energy and the total energy, the same phenomena are observed.

Structure analysis

To investigate deep inside what happened during the temperature and pH change, we need to take a closer look of the protein structure change.

First, we compared the structure of the whole protein at 37 °C at two pH values after simulation of 50 ns. The structures after alignment are shown in Fig. 23. Figure 24 shows the structures after alignment of the whole protein at

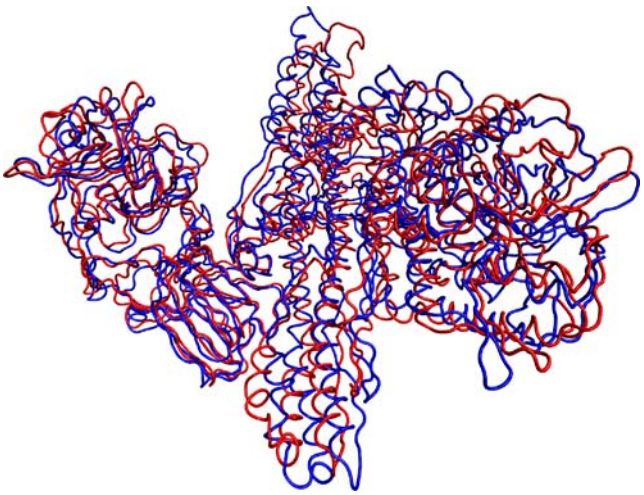

Fig. 23 Structures of BoNT/A at different pH and 37 °C; *red* pH=4.7; *blue* pH=7.0

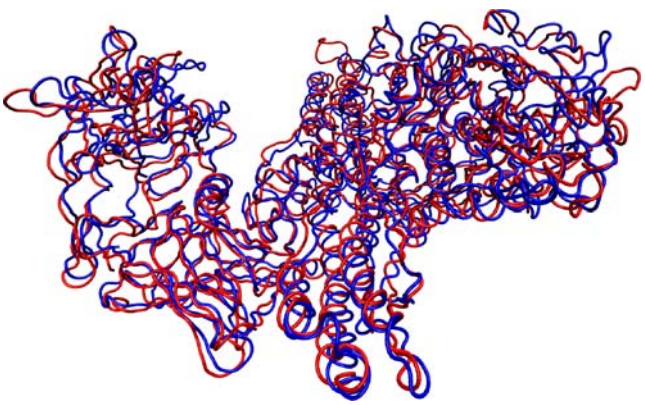

Fig. 24 Structures of BoNT/A at different pH and 55 °C; *red* pH=4.7; *blue* pH=7.0

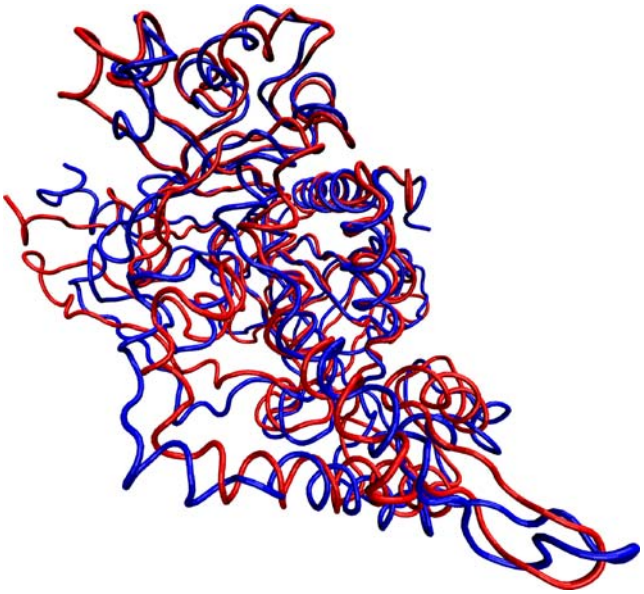

Fig. 25 Structures of LC at different pH and 37 °C; *red* pH=4.7; *blue* pH=7.0

55 °C at two pH values after 50 ns. We can see that the BoNT/A structures are more curled at this high temperature.

The structures after alignment for the LC only runs after 190 ns are shown in Fig. 25 for 37 °C and Fig. 26 for 55 °C. Because the pH change has a significant effect on the energy and structure on the LC, we need an in-depth analysis for the individual HIS residue whole protonation state changes with pH at the atom-level.

BoNT/A is believed to be a zinc endopeptidase [25] that contains the consensus sequence HEXXH (residues 222–226) in the LC. Its crystal structure supports a model in which the HIS222, HIS226, and GLU261 of the HEXXH motif directly coordinate the zinc, and GLU223 coordinates

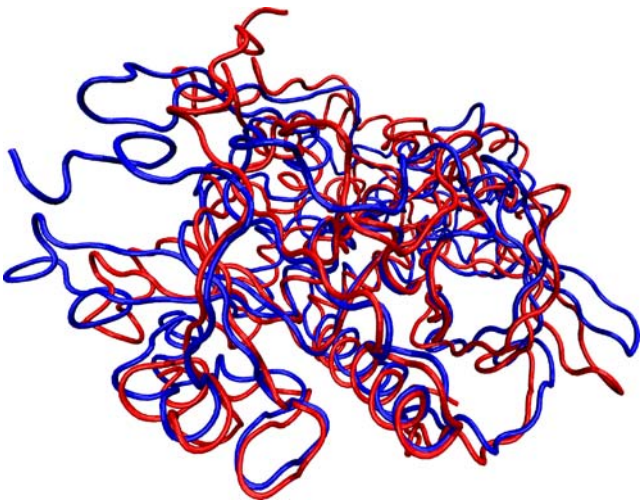

Fig. 26 Structures of LC at different pH and 55 °C; *red* pH=4.7; *blue* pH=7.0

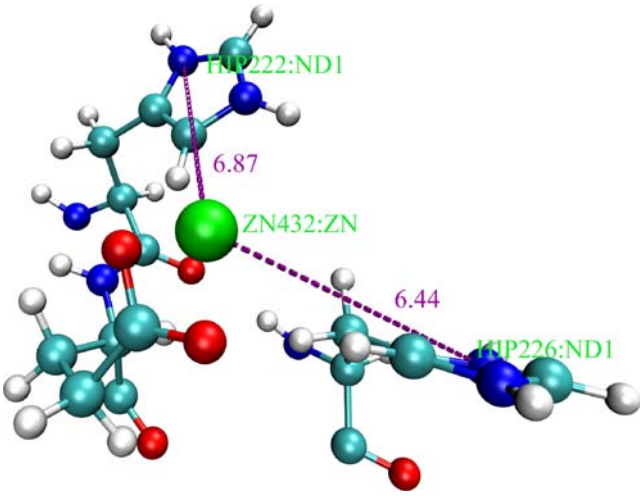

Fig. 27 Coordination between the zinc ion and HIS222 and HIS226 at pH 4.7, 37 °C

a water molecule as the fourth ligand [15, 26]. Since the zinc atom is coordinated with three amino acid residues and an activated water molecule (nucleophilic water), its role is thought to be catalytic [27, 28]. Results show the critical importance of the presence of zinc ion in the cleaving progress of SNAP-25 [25].

There are results which also show the structure of BoNT/B at various pH values ranging from 4 to 7 [29]. This research suggested that, at a low pH environment, the coordination may be lost, but the zinc ion retains its catalytic function. Figures 27 and 28 shows the coordination between the zinc ion and HIS222 and HIS226 at pH 4.7 and 7.0 and 37 °C. Figures 29 and 30 show the coordination between the zinc ion and HIS222 and

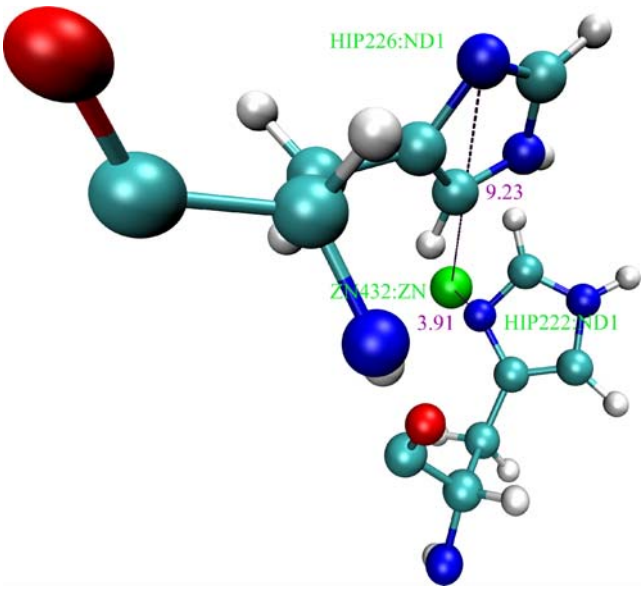

Fig. 28 Coordination between the zinc ion and HIS222 and HIS226 at pH 7.0, 37 °C

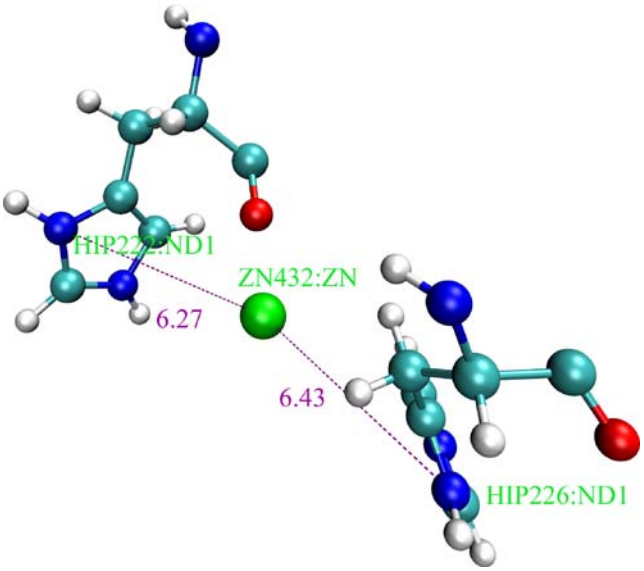

Fig. 29 Coordination between the zinc ion and HIS222 and HIS226 at pH 4.7, 55 °C

HIS226 at pH 4.7 and 7.0 and 55°C. From these figures, we found that, at both temperatures, the protonated histidine residue with +1 charge will repel the zinc ion, which confirm S. Eswaramoorthy's experimental results [29], but the zinc ion remains at its location during the simulation.

Discussions and conclusions

Although the conformational changes usually take a time of the order of a microsecond to occur, our simulations of time 200 ns appear to have shown some interesting results that are consistent with laboratory experiments. Certainly, more conformational changes will emerge if and when one can run for longer time scale.

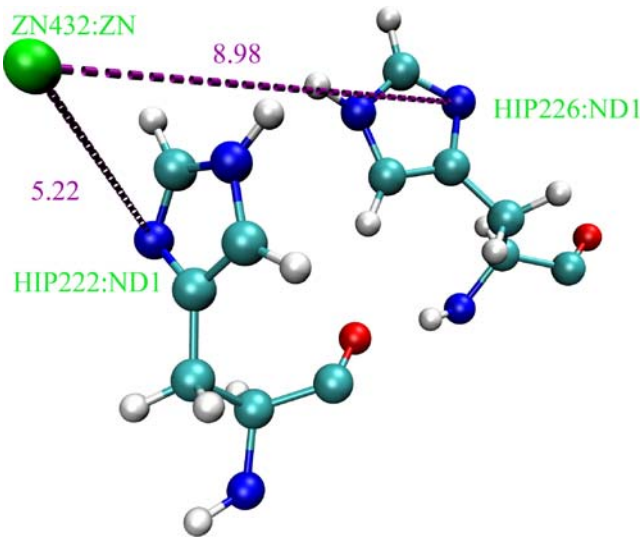

Fig. 30 Coordination between the zinc ion and HIS222 and HIS226 at pH 7.0, 55 °C

Acknowledgements This work was supported by J. Davenport in the Brookhaven National Laboratory by a grant under contract #84054 and the Army Research Office grants #W911NF0510413.

References

1. Singh BR (2000) Nat Struct Biol 7:617–619
2. Arnon SS, Schechter R, Inglesby TV, Henderson DA, Bartlett JG, Ascher MS, Eitzen E, Fine AD, Hauer J, Layton M, Lillibridge S, Osterholm MT, O'Toole T, Parker G, Perl TM, Russell PK, Swerdlow DL, Tonat K (2001) JAMA 285(8):1059–1070
3. Shukla HD, Sharma SK (2005) Crit Rev Microbiol 31(1):11–18
4. Silveira-Moriyama L, Goncalves LR, Maria-Santos A, Chien HF, Barbosa ER (2004) Mov Disord 19:S98–S99
5. Han SH, Lew H, Jeong CW, Lee JB (2001) J Pediatr Ophthalmol Strabismus 38(2):68–71
6. Benedetto AV (1999) Int J Dermatol 38(9):641–655
7. Brashear A, Hogan P, Wooten-Watts M, Marchetti A, Magar R, Martin J (2005) Adv Ther 22(1):49–55
8. Damrose JF, Goldman SN, Groessl EJ, Orloff LA (2004) J Voice 18(3):415–422
9. Porta M, Maggioni G (2004) J Neurol 251:15–18
10. Deng Y, Korobka A, Xiang B (Accepted) Int. J High Perf Comp App
11. Mongan J, Case DA, McCammon AJ (2004) J Comput Chem 25:2038–2048
12. Pearlman DA, Case DA, Caldwell JW, Ross WR, Cheatham TE, DeBolt S, Ferguson D, Seibel G, Kollman P (1995) Comp Phys Commun 91:1–41
13. Li L, Singh BR (2000) Biochemistry 39:6466–6474
14. Swaminathan S, Eswaramoorthy S (2000) Nat Struct Biol 7:693–699
15. Lacy DB, Tepp W, Cohen AC, DasGupta BR, Stevens RC (1998) Nat Struct Biol 5:898–902
16. Berman HM, Westbrook J, Feng Z, Gilliland G, Bhat TN, Weissig H, Shindyalov IN, Bourne PE (2000) Nucleic Acids Res 28:235–242
17. Kalé L, Skeel R, Bhandarkar M, Brunner R, Gursoy A, Krawetz N, Phillips J, Shinozaki A, Varadarajan K, Schulten K (1999) J Comput Phys 151:283–312
18. Ponder JW, Case DA (2003) Adv Prot Chem 66:27–85
19. Humphrey W, Dalke A, Schulten K (1996) J Molec Graphics 14:33–38
20. Zagrovic B, Sorin EJ, Pande V (2001) J Mol Biol 313:151–169
21. Pitera JW, Swope W (2003) Understanding folding and design: replica-exchange simulations of "Trp-cage" miniproteins In: Peter GW (eds) Proceedings of the National Academy of Sciences, San Jose, CA 2003 (100(13):7587–7592)
22. Zagrovic B, Snow CD, Shirts MR, Pande VS (2002) J Mol Biol 323:927–937
23. Ahmed SA (2001) J Protein Chem 20:221–231
24. Lebeda FJ, Olson MA (1994) Proteins 20:293–300
25. Li L, Binz T, Niemann H, Singh BR (2000) Biochemistry 39 (9):2399–2405
26. Schiavo G, Rossetto O, Santucci A, DasGupta BR, Montecucco C (1992) J Biol Chem 267(33):23479–23483
27. Hooper NM (1994) FEBS Lett 354(1):1–6
28. Vallee BL, Auld DS (1990) Biochemistry 29:5647–5659
29. Eswaramoorthy S, Kumaran D, Keller J, Swaminathan S (2004) Biochemistry 43(8):2209–2216